Electronic Supplementary Material (ESI) for Chemical Communications.
This journal is © The Royal Society of Chemistry 2017

Supplementary Information

Wide Graphene Nanoribbons Produced by Intermolecular Fusion of Poly(*p*-phenylene) via Two-Zone Chemical Vapor Deposition

Shaotang Song, Takahiro Kojima, Takahiro Nakae and Hiroshi Sakaguchi*
Institute of Advanced Energy, Kyoto University, Uji, Kyoto 611-0011, Japan

sakaguchi@iae.kyoto-u.ac.jp

Two-zone chemical vapor deposition (2Z-CVD)

The 2Z-CVD system consisted of a quartz tube (ϕ 26 mm, 86 cm) as the reactor; a rotary pump; which can evacuate the system to less than 7×10^{-4} Torr; a two-zone electric furnace with a temperature controller; an Ar gas flow system with a mass-flow controller; and a mantle heater for evaporating the monomer. The quartz tube was cleaned by annealing at 1000 °C for 20 min for removing impurities, which deactivates radicals. The precursor (40 µg, prepared by casting a 120 µL solution, 0.33 mg·mL^{-1} in $CHCl_3$) in a quartz boat and the Au(111)-deposited mica or glass substrate were placed in the quartz tube. Second, Ar was fed into the quartz tube at a flow rate of 500 sccm, resulting in a vacuum of 1 Torr. GNRs were synthesized in two steps: First, the temperature of the quartz tube (zone 2) was set to 250 °C, with the subsequent evaporation of the precursors by heating to approximately 245 °C using the mantle heater. The path of the monomers through the quartz tube (zone 1) was heated to 350 °C; in the second stage, the temperature of zone 2 was increased for converting the polymers into GNRs by interchain fusion.

Scanning tunneling microscopy (STM)

STM measurements were performed in the current-constant mode using a commercial instrument (PicoSPM; Keysight Technologies Inc., formerly Molecular Imaging) under Ar at room temperature.[1] All STM images were recorded at a tip bias of 0.2 V and a constant current of 5–20 pA. An electrochemically etched Pt–Ir (80:20) wire was used as the tip.

Raman spectroscopy

Raman spectra were recorded using a laser Raman microscope (LV-RAM500/532; Lambda Vision Inc.) with a laser emitting at 532 nm. A 0.75/50× microscope objective was used. The diameter of the laser spot is considered in the order of 1 µm. Raman spectra were taken from the different spots of the same sample annealed at different temperatures. Overall, we recorded a spectrum three times for each sample at different positions. The typical Raman integration time was 10 s. The spectra showed a good reproducibility.

Au(111) substrates

Au(111)-deposited glass and mica substrates were prepared using an e-beam vacuum-deposition system. Evaporated gold was deposited on the mica or glass substrate, which was heated at 350 °C under a vacuum of 2×10^{-8} Torr. Deposition was performed at a rate of 0.5 $\text{Å}s^{-1}$, up to a thickness of 30 nm.

Fabrication of field-effect transistor (FET) and measurements

Preparation of a hydrophobic SiO_2/Si substrate

Heavily doped n^{++} silicon substrates with a 300 nm thick SiO_2 gate insulator (SiO_2/Si) were converted into a hydrophobic surface as follows: First, SiO_2/Si substrates were immersed in a mixture of an ammonia solution (1.0 mL, 28 w/w% in water), hydrogen peroxide (1.0 mL, 30w/w% in water), and 5 mL deionized water at 80 °C for 20 min, rinsed with deionized water, dried at 150 °C for 20 min, and irradiated by deep UV light for 15 min. Second, the substrates were immersed in an anhydrous toluene (4.0 mL) solution of chlorotrimethylsilane (40 μL) at 60 °C for 2 h in a glove box, rinsed with toluene (4 mL × 3), and dried at 150 °C for 10 min.

GNR transfer

The GNR/Au(111) glass substrate was immersed in water for separating the GNR/Au(111) film from the glass. Next, the GNR/Au(111) film was placed on the surface of a gold-etchant aqueous solution (10 mL), which contains KI (1.8 g) and I_2 (120 mg). Most of the gold film disappeared after 2 min, and SiO_2/Si was attached to the floating GNRs film. Another 4 min was required for completely etching gold, the GNR-transferred SiO_2/Si was withdrawn from the etchant solution, rinsed with deionized water, a saturated Na_2SO_3 aqueous solution (10.0 g Na_2SO_3 dissolved in 9.0 mL deionized water), and deionized water, followed by drying on a hot plate at 120 °C for 20 min. Finally, GNRs on the SiO_2/Si substrate were annealed in a UHV chamber at 200 °C under a pressure of $<10^{-8}$ Torr for 1 h to strengthen the adhesion of GNRs to the substrate.

FET fabrication

FETs were fabricated by electron-beam lithography using a JEOL JSM-7001 system equipped with BEAM DRAW (Tokyo Technology) at an acceleration voltage of 30 keV. A Pd pad electrode pattern (100 nm thickness, 200 μm × 200 μm pad, 50 μm gap) was deposited on the transferred GNR film via a mask (VECO 100 mesh Cu grid) by vacuum deposition. The GNR film on SiO_2/Si was scratched off by an electrochemically sharpened Pt–Ir (80:20) needle, affording isolated channels. To avoid the current leakage, the insulating mask pattern, except the channels, was prepared by electron-beam lithography on a negative resist (4-methyl-1-acetoxycalix[6]arene, a 2 wt%

chlorobenzene solution) and development by chlorobenzene. The Pd gap electrode pattern was prepared by electron-beam lithography on a spin-coated positive resist (ZEP520A), palladium metal deposition (10.0 nm), and lift-off by the immersion in *N*-methyl-2-pyrrolidone.

I–V measurements

FET devices were set in a vacuum chamber (5×10^{-6} Torr) of a three-terminal probe station. All electrical measurements were performed using a semiconductor characterization system (4200-SCS; Keithley Instruments Inc.) at room temperature. Carrier mobilities were calculated according to the equation used for transconductance measurements.[2]

$$\mu = \left(\frac{L}{W}\right)\frac{1}{C}\frac{1}{V_{DS}}\left(\frac{\partial I_{DS}}{\partial V_{GS}}\right)$$

Here, L and W denote the length (1 μm) and width (500 nm) of the source and drain electrodes, respectively. C denotes the capacitance of 300 nm thick SiO_2 dielectrics (11.6 n Fcm^{-2}).[3] V_{DS} (-30 V) denotes the drain–source voltage. I_{DS} denotes the drain–source current. V_{GS} denotes the gate–source voltage.

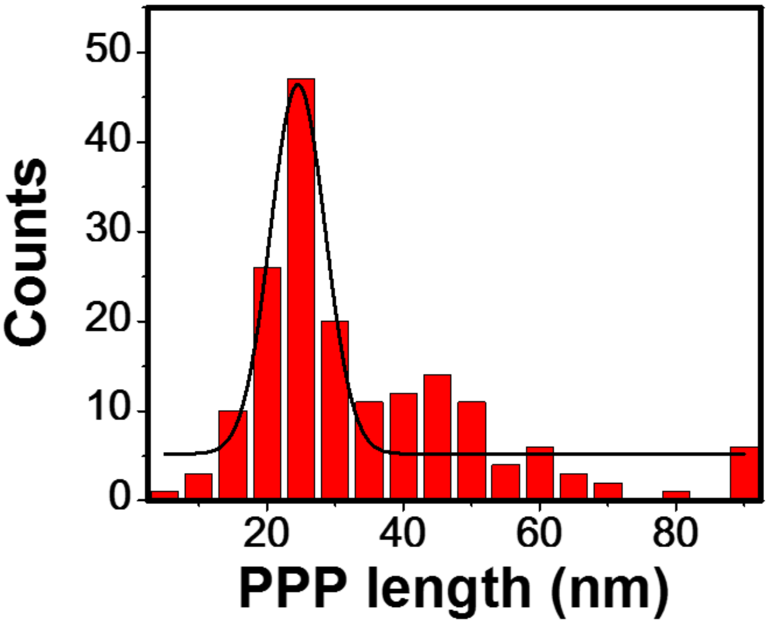

Figure S1. Histogram of PPP chains length distribution from two different samples including Fig. 2a.

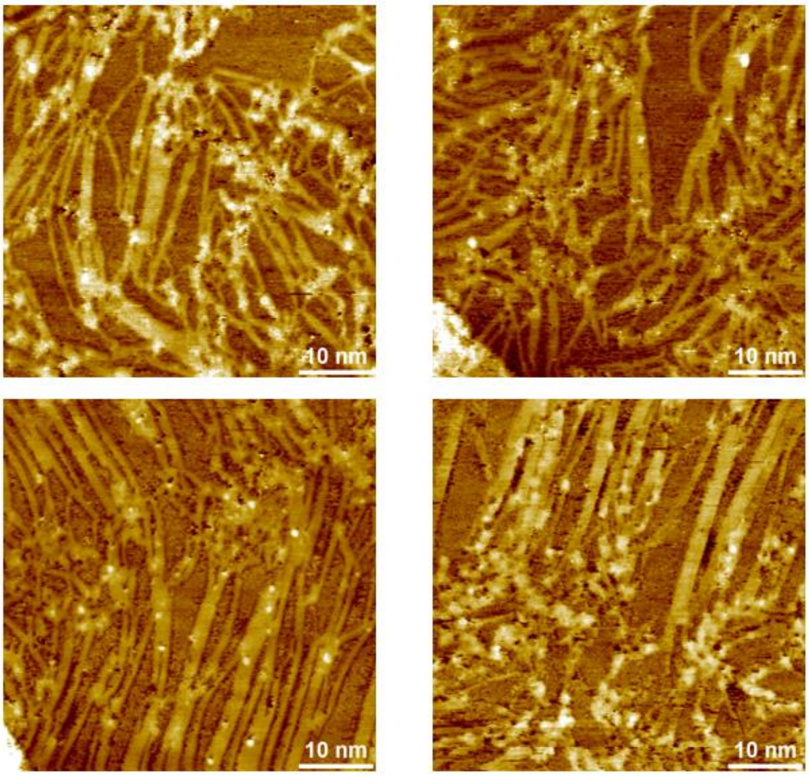

Figure S2. STM images of GNRs on Au(111) at different position after annealing at 600 °C which are used for statistical analysis in Figure 3a.

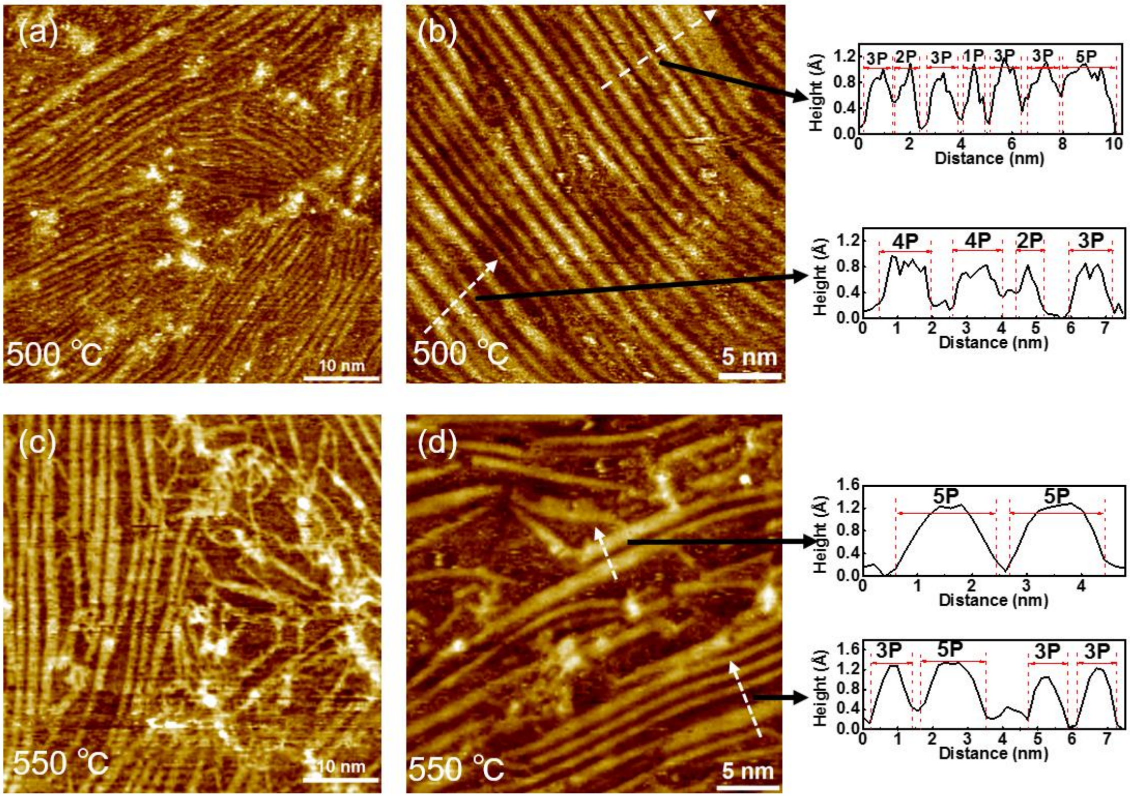

Figure S3. STM images of PPP annealed at 500 °C (a and b) and 550 °C (c and d). Cross sectional analysis of the line in (b and d) indicating the number of fused PPP chains (denoted by *nP*)

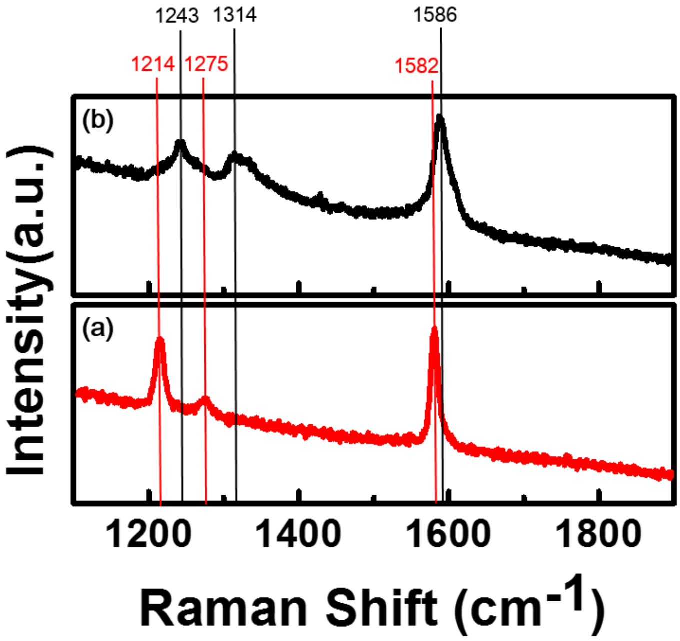

Figure S4. Raman spectra of the materials grown by 2Z-CVD on Au(111) supplied with 40 µg of the DBTP precursor. (a) PPP chains produced at 250 °C. (b) GNRs annealed at 600 °C on Au(111). The three intense peaks between 1200 and 1600 cm^{-1} are associated with the edge C-H in-plane bending mode (~1220 cm^{-1}), the inter-ring C-C stretching mode (~1280 cm^{-1}) and the ring C-C stretching mode (~1600 cm^{-1}).

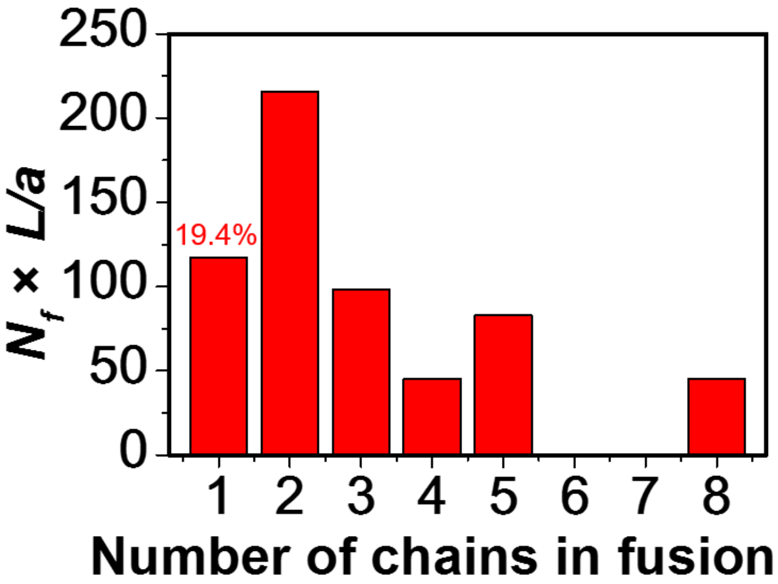

Figure S5. Histogram of chains in fusion distribution based on Fig. 2d, which indicate 19.4% PPP chains remain after annealing at 600 °C.

Table S1. Calculated width of the reported GNRs fabricated by the bottom-up routes.

Chemical Structure	***Calcd. width***
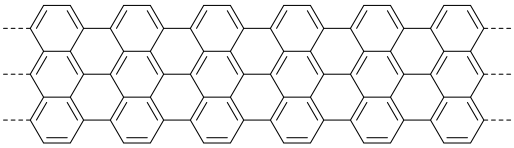	***~1.19 nm***[4]
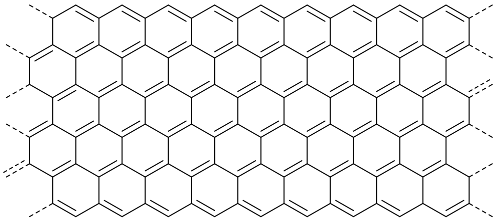	***~1.64 nm***[5]
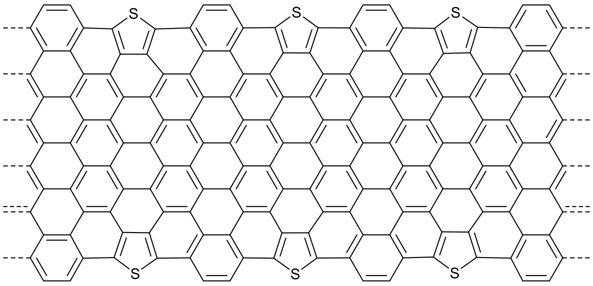	***~1.91 nm***[6]
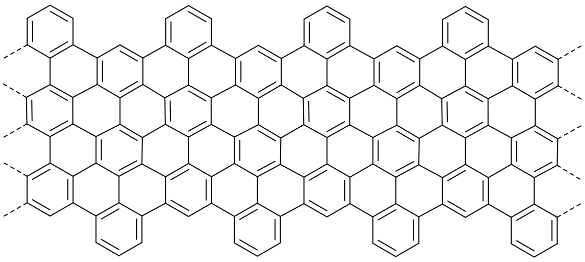	***~1.82 nm***[7]
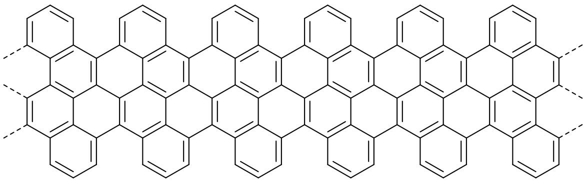	***~1.41 nm***[8]
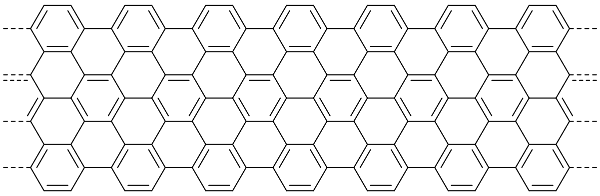	***~1.43 nm***[9]

Reference

1. H. Sakaguchi, H. Matsumura, H. Gong and A. M. bouelwafa, *Science*, 2005, **310**, 1102.
2 S. J. Kang, C. Kocabas, T. Ozel, M. Shim, N. Pimparkar, M. A. Alaam, S. V. Rotkin and J. A. Rogers, *Nat. Nanotech.*, 2007, **2**, 230.
3 D. B. Farmer, Y.-M. Lin and P. Avouris, *Appl. Phys. Lett.*, 2010, **97**, 013103.
4. J. Cai, P. Ruffieux, R. Jaafar, M. Bieri, T. Braun, S. Blankenburg, M. Muoth, A. P. Seitsonen, M. Saleh, X. Feng, K. Müllen and R, Fasel, *Nature*, 2010, **466**, 470.
5. P. Ruffieux, S. Wang, B. Yang, C. Sánchez-Sánchez, J. Liu, T. Dienel, L. Talirz, P. Shinde, C. A. Pignedoli, D. Passerone, T. Dumslaff, X. Feng, K. Müllen and R. Fasel *Nature*, 2016, **531**, 489.
6. G. D. Nguyen, F. M. Toma, T. Cao, Z. Pedramrazi, C. Chen, D. J. Rizzo, T. Joshi, C. Bronner, Y.-C. Chen, M. Favaro, S. G. Louie, F. R. Fischer and M. F. Crommie, *J. Phys. Chem. C.* 2016, **120**, 2684.
7. H. Sakaguchi, S. Song, T. Kojima and T. Nakae, *Nat. Chem.*, 2017, **9**, 57.
8. J. Liu, B. Li, Y.-Z. Tan, A. Giannakopoulos, C. Sanchez-Sanchez, D. Beljonne, P. Ruffieux, R. Fasel, X. Feng and K. Müllen, *J. Am. Chem. Soc.*, 2015, **137**, 6097.
9. L. Talirz, H. Söde, T. Dumslaff, S. Wang, J. R. Sanchez-Valencia, J. Liu, P. Shinde, C. A. Pignedoli, L. Liang, V. Meunier, N. C. Plumb, M. Shi, X. Feng, A. Narita, K. Müllen, R. Fasel and P. Ruffieux, *ACS Nano*, 2017, **11**, 1380.